J Physiol (2003), **550.1**, *pp.* 181–189
DOI: 10.1113/jphysiol.2003.043273

www.jphysiol.org

Journal of Physiology

Interaction between excitatory and inhibitory metabotropic pathways in the guinea-pig antrum

N. Teramoto* and G. D. S. Hirst

*Department of Zoology, University of Melbourne, Victoria, 3010, Australia and * Department of Pharmacology, Graduate School of Medical Sciences, Kyushu University, Fukuoka, 812-8582, Japan*

Intracellular recordings were made from isolated bundles of the circular muscle layer of guinea-pig gastric antrum and the responses evoked by stimulating nitrergic nerve fibres were examined. Nitrergic inhibitory junction potentials (nitrergic-IJPs), evoked by trains of stimuli, had small amplitudes and were associated with a reduction in the rate of occurrence and amplitude of spontaneously occurring depolarizing potentials, termed unitary potentials. Nitrergic-IJPs were abolished either by membrane hyperpolarization or by 4,4′-diisothiocyano-2,2′-stilbene disulfonic acid (DIDS); both of these abolished the discharge of unitary potentials. Membrane depolarization increased the rate of discharge of unitary potentials so that they summed to give rise to a regenerative potential. Nitrergic nerve stimulation abolished regenerative potentials; this inhibition did not result from a change in threshold for the initiation of regenerative potentials, rather it occurred at some stage after the gating process. Inhibitory nitrergic nerve responses were blocked by L-nitroarginine (NOLA) and oxadiazolo quinoxalin-1-one (ODQ), an inhibitor of soluble guanylate cyclase. The observations suggest that the inhibition of regenerative potentials results from an interaction between an inhibitory and an excitatory metabotropic pathway.

(Resubmitted 18 March 2003; accepted after revision 11 April 2003; first published online 9 May 2003)
Corresponding author G. D. S. Hirst: Department of Zoology, University of Melbourne, Victoria, 3010, Australia.
Email: d.hirst@zoology.unimelb.edu.au

In the gastrointestinal tract, slow waves are initiated by a network of interstitial cells of Cajal, which usually lie in the myenteric region (ICC_{MY}) (Ward *et al.* 1994). In the gastric antrum, ICC_{MY} generate pacemaker potentials which passively depolarize the adjacent longitudinal and circular muscle layers (Dickens *et al.* 1999; Hirst & Edwards, 2001; Hirst *et al.* 2002*a*). In the circular layer, each wave of depolarization triggers the secondary regenerative component of the slow wave (Ohba *et al.* 1975; Dickens *et al.* 1999). The secondary component of the slow wave is initiated by intramuscular ICC (ICC_{IM}) and is absent in antral tissues devoid of ICC_{IM} (Dickens *et al.* 2001; Hirst *et al.* 2002*a*). Intramuscular interstitial cells, isolated from the urethra, generate spontaneous transient inward currents (STICs) which result from the release of Ca^{2+} from IP_3-dependent calcium stores and the subsequent activation of calcium-activated chloride channels (Sergeant *et al.* 2001*a*,*b*). Bundles of circular muscle, isolated from the gastric antrum contain both smooth muscle cells and ICC_{IM} (Suzuki & Hirst, 1999). Recordings from such preparations show a discharge of membrane noise. When preparations were bathed in solutions containing BAPTA-AM, so as to buffer the internal concentration of Ca^{2+}, $[Ca^{2+}]_i$, to low levels, the membrane noise was found to result from a high frequency discharge of spontaneous depolarizing potentials, termed unitary potentials (Edwards *et al.* 1999). Like STICs, detected in urethral interstitial cells (Sergeant *et al.* 2001*a*,*b*), antral unitary potentials result from Ca^{2+} release from IP_3-dependent calcium stores and the activation of calcium-activated chloride channels (Hirst *et al.* 2002*b*). Unitary potentials are generated by ICC_{IM}, rather than by smooth muscle cells, since they are absent in tissues which lack ICC_{IM} (Dickens *et al.* 2001; Beckett *et al.* 2002; Suzuki *et al.* 2003). When bundles of antral circular muscle are depolarized, the rate of discharge of unitary potentials rapidly but transiently increases so that unitary potentials sum to give a regenerative potential (Suzuki & Hirst, 1999; Edwards *et al.* 1999; van Helden *et al.* 2000). Again regenerative potentials are generated by ICC_{IM} as they are not evoked by depolarizing bundles of circular muscle devoid of ICC_{IM} (Suzuki *et al.* 2003).

Gastric contractions are influenced by excitatory and inhibitory nerve activity. In the mouse stomach, ICC_{IM} form part of the pathway by which neural information is transferred to smooth muscle cells, with responses to either inhibitory or excitatory nerve stimulation being attenuated in fundal or antral tissues devoid of ICC_{IM} (Burns *et al.* 1996; Ward *et al.* 2000; Beckett *et al.* 2002; Suzuki *et al.* 2003). In many regions of the gut, inhibitory nerve stimulation evokes a biphasic inhibitory junction potential, consisting of an apamin-sensitive fast IJP which is followed by a small amplitude, long lasting, apamin-

insensitive nitrergic-IJPs (Niel *et al.* 1983; Dalzeil *et al.* 1991; Lyster *et al.* 1992; He & Goyal, 1993; Zhang & Paterson, 2002). In the antrum, where inhibitory nerve stimulation evokes apamin-sensitive and nitrergic components, the nitrergic component is dominant (Dickens *et al.* 2000): again the nitrergic component is absent when ICC_{IM} are absent (Suzuki *et al.* 2003). Paradoxically the apamin-sensitive component, which makes little contribution to the inhibition of contractile activity, is associated with a larger hyperpolarization than is the nitrergic component (Dickens *et al.* 2000).

The present experiments have examined nitrergic neurotransmission in bundles of circular muscle isolated from the gastric antrum of guinea-pigs. Nitrergic nerve stimulation decreased the rate of occurrence and amplitude of unitary potentials and abolished regenerative potentials. The results suggest that neurally released NO causes the formation of cyclic guanylate mono-phosphate, cyclic GMP, which inhibits the IP_3-dependent pathway present in ICC_{IM} both at rest and when further activated during a regenerative potential.

METHODS

The procedures described were approved by the animal experimentation ethics committee at the University of Melbourne. Guinea-pigs of either sex were stunned, exsanguinated and the stomach removed. The antral region was isolated and immersed in oxygenated physiological saline (composition, mM): NaCl, 120; $NaHCO_3$, 25; NaH_2PO_4, 1.0; KCl, 5; $MgCl_2$, 2; $CaCl_2$, 2.5; and glucose, 11; bubbled with 95 % O_2–5 % CO_2. Single bundles of circular muscle (diameter 80–150 μm, length 400–600 μm) were pinned in a recording chamber as described previously (Suzuki & Hirst, 1999). Preparations were impaled with two independent electrodes (resistance 90–150 MΩ, filled with 0.5 M KCl). Intramuscular nerve terminals were stimulated using two platinum stimulating electrodes, positioned on either side of the preparation (Hirst *et al.* 2002*c*). Nifedipine (1 μM), atropine (1 μM) and apamin (0.1 μM) were added to the physiological saline, warmed to 37 °C, to reduce movements and to abolish the effects of stimulating excitatory nerves and of the apamin-sensitive component of the inhibitory nerve response (Hirst *et al.* 2002*c*). The inhibitory responses detected in atropine and apamin were abolished by tetrodotoxin (1 μM; $n = 3$), indicating that they resulted from nerve stimulation. The effects of nitrergic nerve stimulation were assessed in three ways. Since individual traces were dominated by the discharge of membrane noise, the amplitudes of nitrergic-IJPs were determined by averaging some 10–40 successive responses to trains of stimuli. In a group of these preparations, selected because unitary potentials occurred at a low enough frequency for their amplitudes and frequency to be determined directly, their mean amplitudes and frequency were determined from a series of 20 individual traces. Control measurements were made during a 5 s period immediately before the presentation of each train of stimuli and for a 5 s period which coincided with the peak of the averaged nitrergic-IJP. In preparations where unitary potentials occurred at higher frequencies, power spectral density curves were constructed from sets of eight traces collected before and after the trains of stimuli, with each sampling period lasting for 2.5 s (see Suzuki *et al.* 2003).

All data are expressed as means ± standard errors of the mean (S.E.M.). Each n value represents a recording made from a separate preparation taken from a separate animal. Paired Student's t tests were used to determine if data sets differed, with P values < 0.05 taken to indicate significant differences.

L-Nitroarginine (NOLA) (Calbiochem, San Diego, CA, USA), oxadiazolo quinoxalin-1-one (ODQ), 4,4′-diisothiocyano-2,2′-stilbene disulfonic acid (DIDS), apamin, tetrodotoxin and nifedipine (Sigma Chemical Co., St Louis, MO, USA) were used in these experiments.

RESULTS

Properties of nitrergic-IJPs recorded from isolated bundles of the circular layer of guinea-pig antrum

Intracellular recordings were made from electrically short bundles of circular muscle dissected from the antral region, using two independent electrodes, one to pass current and the other to record membrane potential changes (Suzuki & Hirst, 1999). Hyperpolarizing current pulses evoked electrotonic potentials whose time courses could be described by single exponential functions with time constants in the range 85–350 ms (205 ± 20 ms, $n = 17$). Preparations had input resistances in the range 1.5–11.4 MΩ (4.2 ± 0.8 MΩ, $n = 17$) and resting potentials in the range −57 to −69 mV (−63.5 ± 0.7 mV, $n = 17$). Depolarizing current pulses evoked regenerative potentials with peak amplitudes in the range 18.5–38.1 mV (29.6 ± 1.2 mV, $n = 17$). Nitrergic-IJPs, evoked by trains of 10 impulses delivered at 5 Hz and recorded in physiological saline containing nifedipine (1 μM), apamin (0.1 μM) and atropine (1 μM), had peak amplitudes in the range 0.7–3.4 mV (2.1 ± 0.2 mV, $n = 17$). Since individual traces were invariably dominated by discharges of membrane noise, the amplitudes of the responses were determined by averaging some 10–40 successive responses (Fig. 1*A*).

In five preparations the rate of discharge of unitary potentials and their amplitudes at rest and following trains of stimuli were determined directly. These preparations had high input resistances (8.0 ± 1.1 MΩ, $n = 5$): presumably this resulted simply because they had fewer smooth muscle cells and ICC_{IM} than the other preparations, since their mean time constants and resting potentials were not different. In the high resistance preparations unitary potentials occurred at a sufficiently low rate to detect individual events. The results from one experiment, where the effects of nitrergic nerve stimulation on the discharge of unitary potentials were examined, are illustrated in Fig. 1. The time course and amplitude of the nitrergic-IJP was determined from the average of 40 successive trains of stimuli (Fig. 1*A*). However, when individual traces were examined a clear hyperpolarization following the period of nitrergic stimulation could not be detected (Fig. 1*Aa–c*). This suggests that at rest sufficient unitary potentials occur to

give an average depolarization but when the discharge of unitary potentials is suppressed by neurally released NO the mean membrane potential falls to its true resting value. In the experiment shown in Fig. 1, the frequency of unitary potentials fell from 1.21 to 0.45 unitary potentials s^{-1} during the nitrergic-IJP. When amplitude–frequency histograms of the unitary potentials were determined it was found that the mean amplitudes of the unitary potentials had also fallen, in this experiment, from 0.70 to 0.45 mV (Fig. 1*B* and *C*). From the grouped data of the five preparations analysed in this way, the frequency of unitary potentials fell from 1.42 ± 0.14 to 0.55 ± 0.09 unitary potentials s^{-1} ($n = 5$). Using a paired t test these values were significantly different. From the grouped data, the mean amplitudes of the unitary potentials fell from 0.91 ± 0.22 to 0.52 ± 0.15 mV ($n = 5$); again these values were significantly different.

Nitrergic-IJPs were associated with a fall in low power spectral density (Fig. 2*B*; see Suzuki *et al.* 2003). Power spectral density curves were calculated for nine preparations and their theoretical descriptions estimated as described previously (Edwards *et al.* 1999). Satisfactory fits were obtained from control recordings before the trains of stimuli using pairs of time constants A and B in the range 320–600 ms (500 ± 30 ms mV, $n = 9$) and 60–125 ms (80 ± 5 ms mV, $n = 9$), respectively. During nitrergic-IJPs the same time constants provided adequate descriptions of the spectral density curves but the spectral density power fell (Fig. 2*B*): on one occasion no low frequency power that could be attributed to the discharge of unitary potentials was detected during the nitrergic-IJP (see Fig. 3*F*). From the grouped observations, the spectral density fell to 14 ± 11 % of control during the nitrergic-IJP ($n = 9$).

Antral unitary potentials are blocked by agents which block calcium-activated chloride channels (Hirst *et al.* 2002*b*). In the present experiments, DIDS (100 μM) abolished the discharge of membrane noise and produced a hyperpolarization of 4.7 ± 0.9 mV ($n = 4$). At the same

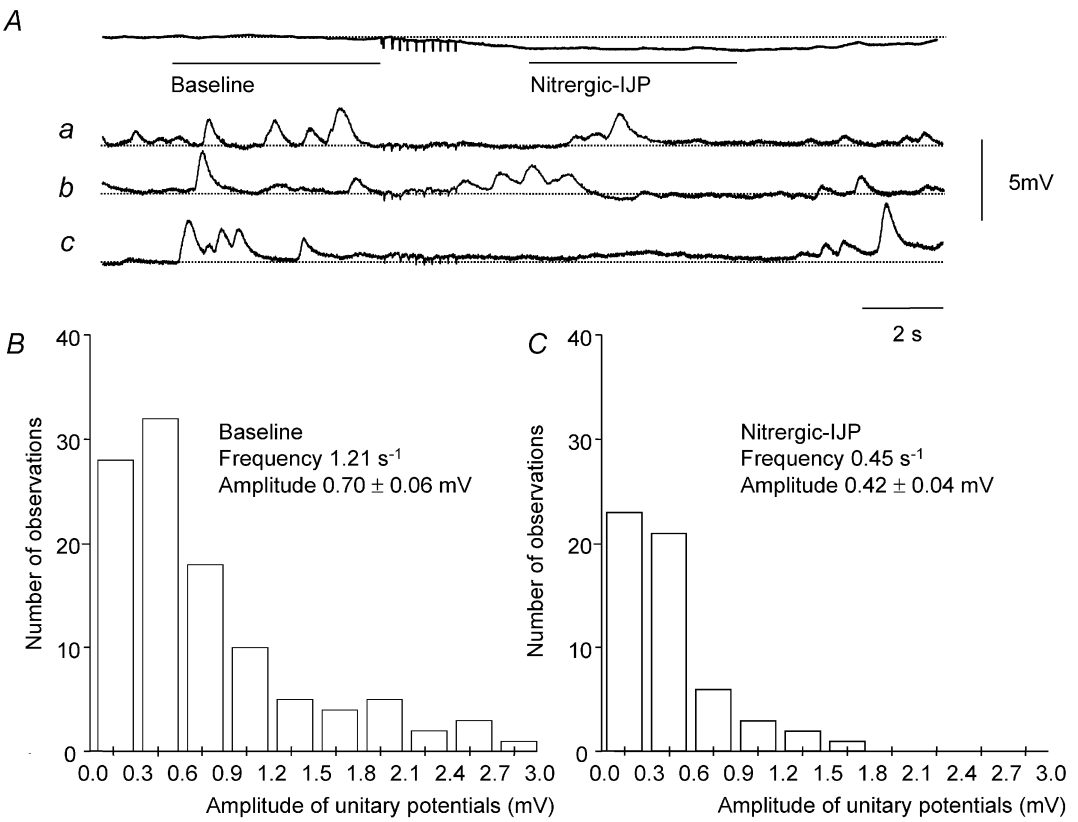

Figure 1. Effect of nitrergic nerve stimulation on the frequency and amplitude of unitary potentials in the circular layer of guinea-pig gastric antrum

A, a train of stimuli (10 impulses at 5 Hz) evoked a nitrergic-IJP with a peak amplitude of 0.7 mV. A sample of three (traces *a–c*) of the 35 individual traces which made up this averaged response is shown below. The rate of occurrence of unitary potentials fell during the nitrergic-IJP from 1.21 to 0.45 s^{-1}. The amplitude frequency histograms of unitary potentials, determined from the baseline period (*B*) and during the nitrergic-IJP (*C*), showed that the mean amplitude of the unitary potentials fell from 0.7 to 0.42 mV. The resting membrane potential was –61 mV(*Aa–c*); in preparations where the frequency of unitary potentials was low this corresponded with the peak hyperpolarization detected during the nitrergic-IJP. Time and voltage calibration bars apply to all recordings. Nifedipine (1 μM), atropine (1 μM) and apamin (0.1 μM) were present throughout.

time nitrergic-IJPs, which had a mean amplitude of 1.3 ± 0.3 mV (n = 4), were abolished (Fig. 2*A* and *C*). The abolition of membrane noise by DIDS, like the nitrergic-IJP, was associated with a decreased discharge of low frequency noise (Fig. 2*B* and *D*).

Together the observations show that in the circular layer of the guinea-pig antrum, nitrergic nerve stimulation causes a small hyperpolarization that can be attributed to a changed discharge of antral unitary potentials and hence a decreased mean chloride conductance, g_{Cl}, generated by ICC_{IM} (Hirst *et al.* 2002*b*). This might imply that nitrergic-IJPs would persist at more negative potentials. However hyperpolarizing the membrane by 15 mV invariably abolished nitrergic-IJPs (Fig. 3*A* and *B*), but more profound hyperpolarization failed to invert them (Fig. 3*C*). When individual membrane potential traces were examined, without nerve stimulation, it became apparent that membrane hyperpolarization had inhibited the discharge of membrane noise (Fig. 3*E*). When the discharge of membrane noise was compared at –60 mV and at –75 mV, hyperpolarization suppressed the discharge of membrane noise (Fig. 3*G*) in a similar way to nitrergic nerve stimulation (Fig. 3*F*). When power spectral density curves were constructed at resting (−61.3 ± 1.3 mV) and at hyperpolarized potentials (−77.3 ± 2.3 mV; n = 4), the spectral density fell to 12 ± 5 % of its control value. Hyperpolarizing the membrane by approximately 5 mV failed to produce a detectable change in the discharge of membrane noise (n = 3), suggesting that the hyperpolarization detected during a nitrergic-IJP resulted from a suppression of membrane noise rather than the converse.

Interaction between nitrergic-IJPs and regenerative potentials

The previous observations suggest that nitrergic-IJPs result from a reduction in the rate of discharge and amplitude of unitary potentials. The following experiments examined

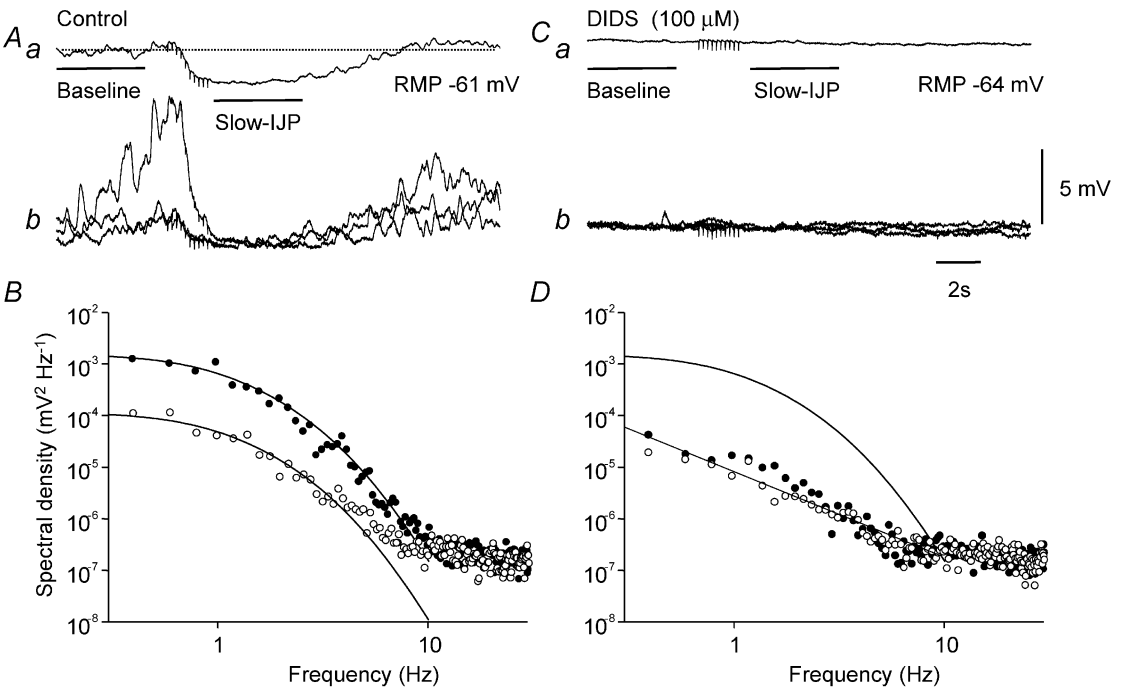

Figure 2. Effect of DIDS on nitrergic-IJPs and discharge of membrane noise in the circular layer of guinea-pig antrum

The upper left trace (*Aa*) shows a nitrergic-IJP, evoked by a train of stimuli (10 impulses at 5 Hz) at resting potential −61 mV, with an amplitude of 2.2 mV. Three of the individual traces that made up the averaged nitrergic-IJP are shown superimposed below (*Ab*). Baseline (●) and nitrergic-IJP (○)regions of these traces were used to calculate the power spectral density curves shown in *B*. Each power spectral curve was adequately fitted using time constants A and B of 515 ms and 60 ms, respectively. The upper right trace (*Ba*) shows the average response, evoked by a train of stimuli (10 impulses at 5 Hz) in the presence of DIDS (100 μM). DIDS caused a baseline membrane potential hyperpolarization of 4 mV and abolished the nitrergic-IJP. Three of the individual traces, which made up the averaged response in DIDS are shown below (*Bb*). Baseline (●) and nitrergic-IJP (○)regions of these traces were used to calculate the power spectral density curves shown in *D*. Note that the residual low frequency power detected in DIDS was abolished by nitrergic nerve stimulation. Also shown in *D*, for comparison, is the control theoretical spectral density curve shown in *A*, determined before the addition of DIDS. Nifedipine (1 μM), atropine (1 μM) and apamin (0.1 μM) were present throughout.

the interaction between nitrergic nerve stimulation and regenerative potentials. Depolarizing current steps initiated regenerative potentials (Fig. 4*Aa*). Trains of stimuli (5–15 impulses at 5 Hz) were presented 1, 2, 3 and 4 s after the start of the depolarizing pulses (Fig. 4*Af*) used to initiation the regenerative potentials. When presented just as a regenerative potential was initiated, the regenerative potential was abolished (Fig. 4*Ab*). When stimuli were presented after a regenerative potential had started, the regenerative potential was abruptly terminated (Fig. 4*Ac–e*).

When the intensity of depolarizing current was increased from its threshold value (Fig. 4*Ba*), nitrergic nerve stimulation continued to abolish regenerative potentials (Fig. 4*Bb*; $n = 6$). Regenerative potentials can be triggered by brief depolarizing pulses even though the membrane potential returns towards its resting value before the regenerative potential is initiated (Fig. 4*Ca*; Suzuki & Hirst, 1999). When brief trains of stimuli (five impulses at 10 Hz) were applied during the latent period, they also abolished regenerative potentials (Fig. 4*Cb*).

Nitrergic inhibition of regenerative potentials was abolished by NOLA (10 μM; Fig. 5*A*). The amplitude of control regenerative potentials was 27.5 ± 1.4 mV (see Fig. 5*Aa*); during nerve stimulation electrotonic potentials had an amplitude of 8.2 ± 0.2 mV (see Fig. 5*Ab*); in NOLA, regenerative potentials, during nerve stimulation, had a mean amplitude of 27.1 ± 1.3 mV (see Fig. 5*Ac*; $n = 4$). Nitrergic inhibition was also abolished by ODQ, an inhibitor of soluble guanylate cyclase (Fig. 5*B*). The amplitude of the control regenerative potentials was 31.8 ± 2.6 mV (see Fig. 5*Ba*); during nerve stimulation the amplitude of electrotonic potentials was 7.9 ± 1.5 mV(see Fig. 5*Bb*); in ODQ, 1 μM, regenerative potentials, during nerve stimulation, had an amplitude of 32.0 ± 2.7 mV (see Fig. 5*Bc*); $n = 4$. NOLA ($n = 4$) and ODQ ($n = 4$) each abolished nitrergic-IJPs.

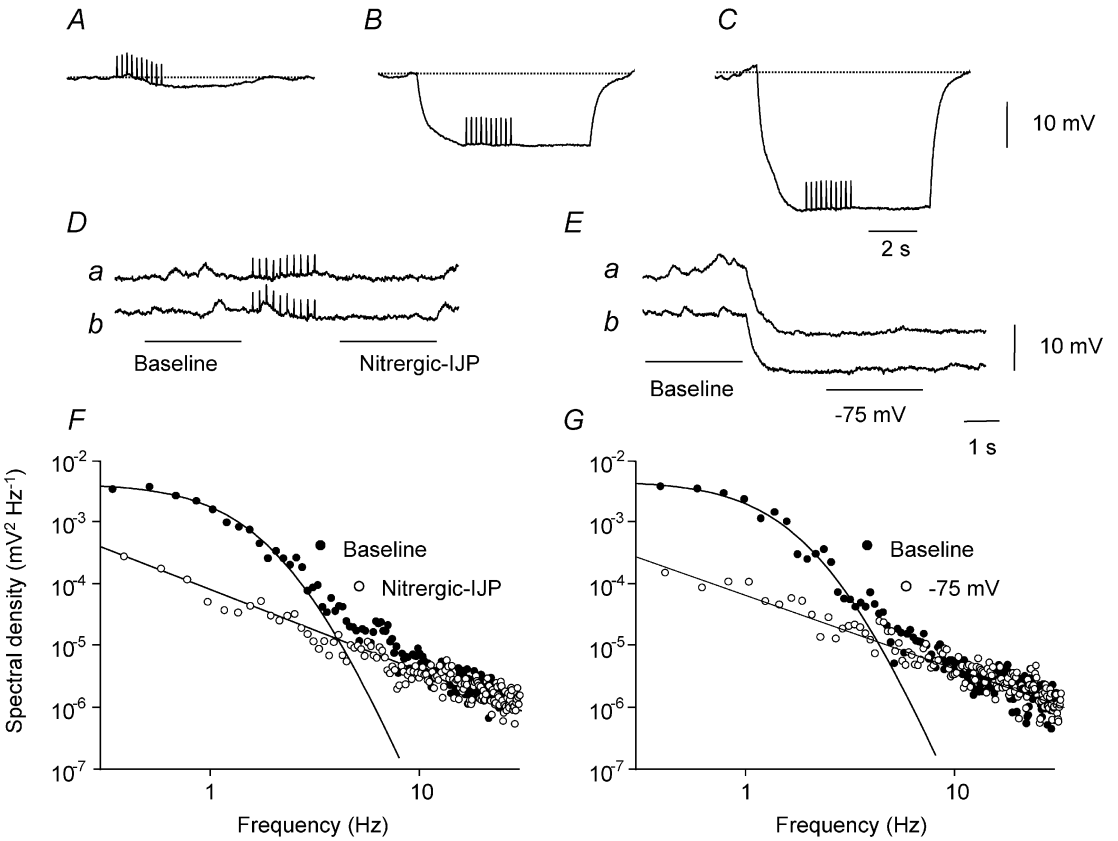

Figure 3. Effect of changing membrane potential on nitrergic-IJPs recorded from the circular layer of guinea-pig antrum

The upper three traces show a nitrergic-IJP, evoked by a train of stimuli (10 impulses at 5 Hz) at resting potential, −61 mV, with an amplitude of 2.7 mV (*A*), during a hyperpolarizing current pulse, 2 nA (*B*) and during a hyperpolarizing current pulse, 4 nA (*C*): each trace is an average of 10 successive trials. Two of the individual traces, which made up the averaged nitrergic-IJP are shown below (*Da* and *b*). Baseline (●) and nitrergic-IJP (○) regions of these traces were used to calculate the power spectral density curves shown in *F*. Power at low frequencies was not detected during the nitrergic-IJP. The middle right traces (*Ea* and *b*) show two of the traces used to calculate the power spectral curves at –61 mV and at –75 mV shown in *G*. Note that at a membrane potential of –75 mV, power at low frequencies was absent. Nifedipine (1 μM), atropine (1 μM) and apamin (0.1 μM) were present throughout.

DISCUSSION

The experiments show that nitrergic nerve stimulation abolishes regenerative potentials in the circular muscle layer of the gastric antrum of guinea-pigs. Regenerative potentials involve Ca^{2+} release from IP_3-dependent stores, presumably associated with membrane potential-dependent formation of IP_3 in ICC_{IM}. On the other hand nitrergic inhibition involved the formation of cyclic GMP, with the interaction between the two pathways appearing to occur at an intracellular level.

Nitrergic-IJPs were associated with a fall in the rate of discharge of unitary potentials (Fig. 1). When successive traces were averaged, this gave rise to a long lasting hyperpolarization with a peak amplitude of about 3 mV, which was only apparent on the averaged response. This suggests that nitrergic-IJPs result solely from a suppression of unitary potentials rather than from activation of a hyperpolarizing conductance change. Neurally released NO, as well as reducing the rate of discharge of unitary potentials also reduced their mean size. It is not clear how this might occur. All recordings were made from bundles of circular muscle containing a population of smooth muscle cells and a population of ICC_{IM}. One possibility is that individual ICC_{IM} each discharge unitary potentials of fixed size and those discharging larger signals are preferentially inhibited by neurally released NO. Alternatively the size of unitary potentials, generated by a given ICC_{IM}, might not be fixed, with neurally released NO changing both the amplitude and frequency of discharge of unitary potentials. This

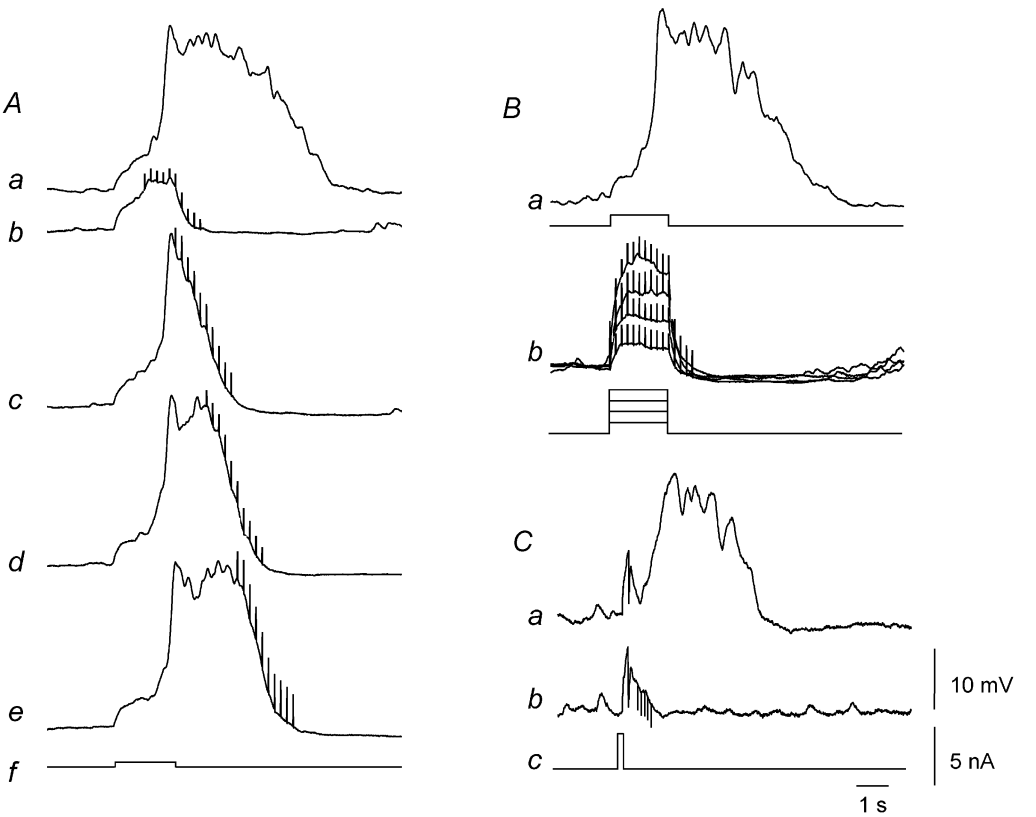

Figure 4. Inhibition of regenerative responses by nitrergic nerve stimulation in the circular layer of guinea-pig antrum

The family of traces shown on the left-hand side of the figure (*Aa–f*) illustrate the effect of nitrergic nerve stimulation on regenerative potentials. A regenerative potential (*Aa*) was evoked by a depolarizing current pulse (*Af*). The regenerative potential was abolished when a train of stimuli (10 impulses at 5 Hz) was applied during the depolarizing current (*Ab*). The duration of the regenerative potential was reduced when the same train of stimuli was applied at progressively later times during the regenerative potential (*Ac–e*). The same current pulse (*Af*) was applied on each occasion. The resting membrane potential was –62 mV. The upper right trace (*Ba*) shows a regenerative potential initiated by a threshold depolarization at resting potential, −69 mV. The lower trace (*Bb*) shows that increasing the amplitude of the depolarizing pulse did not overcome the inhibition produced by nitrergic nerve stimulation. The lower right trace (*Ca*) shows a regenerative potential initiated by a brief depolarizing pulse (*Cc*) at resting potential, −62 mV. The lower trace (*Cb*) shows that a brief train of stimuli (five impulses at 10 Hz) presented during the latent period inhibited the subsequent generation of a regenerative potential. Time, voltage and current calibration bars apply to all recordings. Nifedipine (1 μM), atropine (1 μM) and apamin (0.1 μM) were present throughout.

second possibility seems more likely since successive STICs recorded from isolated urethral interstitial cells vary in size (Sergeant *et al.* 2001*a*,*b*). Moreover when the frequency of unitary potentials was increased by depolarization, an increase in mean amplitude was detected (Edwards *et al.* 1999). In preparations where unitary potentials occurred at high frequency, neurally released NO produced in a fall in low frequency power in the spectral density curves constructed before and after nerve stimulation (Fig. 2). In the mouse antrum nitrergic-IJPs were found to be associated with a decreased variance of the membrane potential and a similar fall in power of the spectral density curves at low frequencies (Suzuki *et al.* 2003). Thus three different measures of the discharge of antral unitary potentials support the view that the hyperpolarization evoked by nitrergic nerve stimulation is associated with inhibition of the discharge of unitary potentials. When antral unitary potentials were abolished by DIDS, nitrergic-IJPs were abolished and an underlying IJP was not detected (Fig. 2). Together these observations suggest that nitrergic-IJPs do not result from an increase in conductance to other ions, presumably potassium ions, g_K, unless that conductance is itself blocked by DIDS: rather they suggest that inhibition of unitary potentials is the basis of the nitrergic-IJP. Since antral unitary potentials result from increases in g_{Cl} (Hirst *et al.* 2002*b*), the present observations are consistent with the view that nitrergic-IJPs result from a suppression of g_{Cl} (Crist *et al.* 1991*a*,*b*; Zhang & Paterson, 2002), located in ICC_{IM} (Burns *et al.* 1996; Suzuki *et al.* 2003).

Nitrergic-IJPs were not detected when the membrane potential was hyperpolarized from about –60 mV to about –75 mV but further hyperpolarization failed to reveal an inverted IJP (Fig. 3). This again suggests that nitrergic-IJPs do not result from an increase in g_K, unless the conductance is inactivated by hyperpolarization. Rather it appeared that nitrergic-IJPs were not detected at hyperpolarized potentials because membrane hyperpolarization inhibited the discharge of antral unitary potentials so

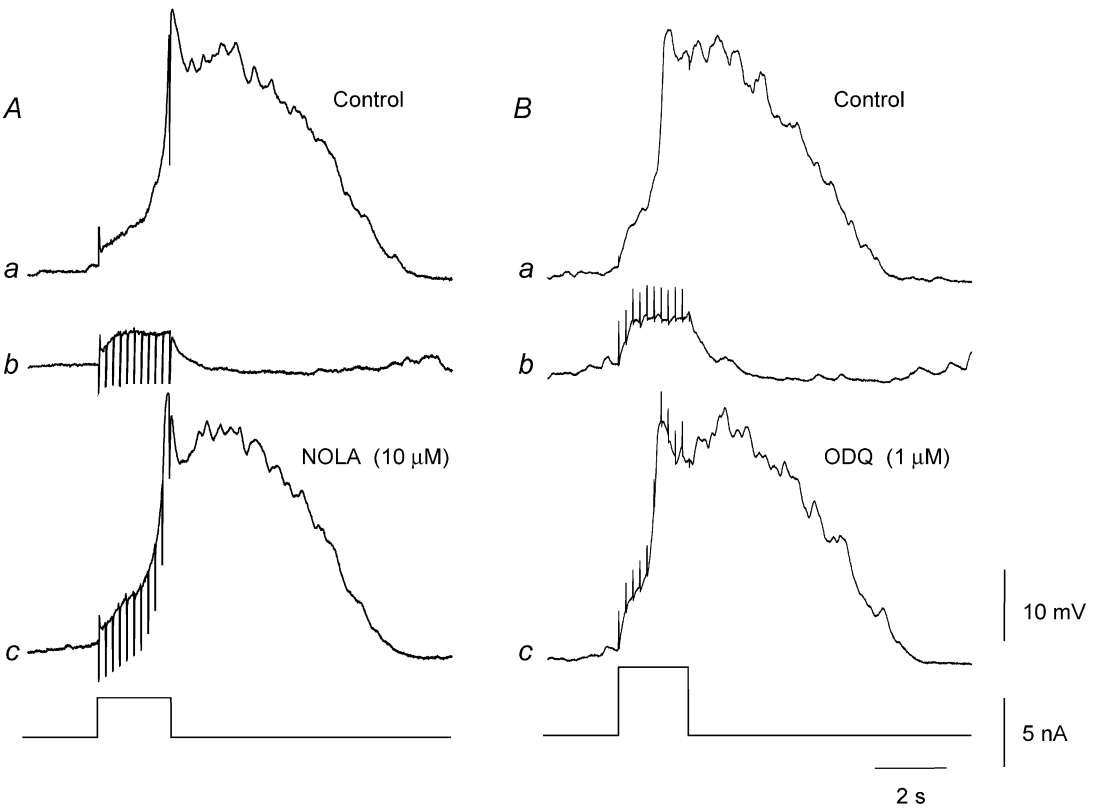

Figure 5. Neurally released NO inhibits regenerative potentials via cyclic-GMP in the circular layer of guinea-pig antrum

The left-hand panels show the effect of NOLA (10 μM) on nitrergic inhibition of regenerative potentials. A regenerative potential (*Aa*) was abolished by nitrergic nerve stimulation (10 impulses at 5 Hz; *Ab*). Fifteen minutes after adding NOLA, the same train of stimuli failed to abolish the regenerative potential (*Ac*); resting potential –62 mV throughout. The right-hand panels show the effect of ODQ (1 μM) on nitrergic inhibition of regenerative potentials. A regenerative potential (*Ba*) was abolished by nitrergic nerve stimulation (10 impulses at 5 Hz; *Bb*). Seven minutes after adding ODQ, the same train of stimuli no longer abolished the regenerative potential (*Bc*); resting potential –64 mV throughout. Time, voltage and current calibration bars apply to all recordings. Nifedipine (1 μM), atropine (1 μM) and apamin (0.1 μM) were present throughout.

removing the target of NO inhibition (Fig. 3). This suggestion is consistent with the view that the discharge of antral unitary potentials depends upon the voltage-dependent production of IP_3 within ICC_{IM} (Suzuki & Hirst, 1999; van Helden *et al.* 2000; Dickens *et al.* 2001). In smooth muscle cells the concentration of IP_3, determined in the presence of an agonist, is reduced by membrane hyperpolarization (Itoh *et al.* 1992); presumably this also occurs in ICC_{IM}. Certainly the same pathway, when activated in ICC_{IM} by neurally released acetylcholine, shows a similar voltage dependency with the responses to excitatory nerve stimulation being abolished by moderate hyperpolarization (Hirst *et al.* 2002*c*).

In the antrum, periods of membrane depolarization cause many unitary potentials to sum to give a regenerative potential (Edwards *et al.* 1999). This is manifest as the secondary component of the antral slow wave (Dickens *et al.* 1999), which is absent in tissues which lack ICC_{IM} (Dickens *et al.* 2001; Hirst *et al.* 2002*a*). Regenerative potentials were abolished by nitrergic nerve stimulation (Fig. 4). This observation indicates that neurally released NO inhibits the discharge of unitary potentials during a regenerative potential. Inhibition occurred at some stage after the gating process: thus inhibition was manifest after a regenerative potential had started, was not overcome by increasing stimulus strength and was effective if applied during the latent period between stimulation and response (Fig. 4). Nitrergic inhibition in the antrum, as has been shown in several intestinal tissues (Ward *et al.* 1992), involved the formation of cyclic GMP, with inhibitory responses being abolished by ODQ (Fig. 5). When the interaction between NO donors and calcium-activated chloride channels was examined in isolated cat tracheal smooth muscle cells, NO donors affected neither the opening of these channels nor any part of the pathway between the release of caged IP_3 and an increase in g_{Cl} (Waniishi *et al.* 1998). However NO donors blocked the pathway activated by applied acetylcholine in a way that involved cyclic GMP (Waniishi *et al.* 1998). If these findings apply to ICC_{IM}, the simplest explanation is that neurally released NO in some way prevents the formation of IP_3 in ICC_{IM}, perhaps through an effect on protein kinase C (see Kito *et al.* 2002).

The observations may in part explain how neurally released NO reduces gastric motility (Dickens *et al.* 2000). The secondary regenerative component of the slow wave ensures that the membrane potential of circular smooth muscle cells moves through a window where L-type Ca^{2+} channels are opened. Neurally released acetylcholine activates the same pathway to trigger a regenerative potential (Hirst *et al.* 2002*c*), with these responses also depending upon the presence of ICC_{IM} (Ward *et al.* 2000; Suzuki *et al.* 2003). Clearly in intact tissues, neurally released NO will also exert an inhibitory effect by blocking both the regenerative component of the slow wave and the effects of neurally released acetylcholine.

In summary, these experiments have shown that in the gastric antrum, neurally released NO selectively inhibits the discharge of unitary potentials by ICC_{IM}. Cyclic GMP is formed and this inhibits the IP_3-dependent pathway activated during a regenerative potential. Thus both the inhibitory and excitatory pathways involve the formation of distinct second messengers and the two messengers appear to interact at a subcellular level.

REFERENCES

Beckett EAH, Horiguchi K, Khoyi M, Sanders KM & Ward SM (2002). Loss of enteric motor neurotransmission in the gastric fundus of *Sl/Sl*(*d*) mice. *J Physiol* **543**, 871–887.

Burns AJ, Lomax AE, Torihashi S, Sanders KM & Ward SM (1996). Interstitial cells of Cajal mediate inhibitory neurotransmission in the stomach. *Proc Natl Acad Sci U S A* **93**, 12008–12013.

Crist JR, He XD & Goyal RK (1991*a*). Chloride-mediated junction potentials in circular muscle of the guinea pig ileum. *Am J Physiol* **261**, G742–751.

Crist JR, He XD & Goyal RK (1991*b*). Chloride-mediated inhibitory junction potentials in opossum esophageal circular smooth muscle. *Am J Physiol* **261**, G752–762.

Dalziel HH, Thornbury KD, Ward SM & Sanders KM (1991). Involvement of nitric oxide synthetic pathway in inhibitory junction potentials in canine proximal colon. *Am J Physiol* **261**, G789–792.

Dickens EJ, Edwards FR & Hirst GDS (2000). Vagal inhibitory projections to rhythmically active cells in the antral region of guinea-pig stomach. *Am J Physiol Gastrointest Liver Physiol* **279**, G388–399.

Dickens EJ, Edwards FR & Hirst GDS (2001). Selective knockout of intramuscular interstitial cells reveals their role in the generation of slow waves in mouse stomach. *J Physiol* **531**, 827–833.

Dickens EJ, Hirst GDS & Tomita T (1999). Identification of rhythmically active cells in guinea-pig stomach. *J Physiol* **514**, 515–531.

Edwards FR, Hirst GDS & Suzuki H (1999). Unitary nature of regenerative potentials recorded from circular smooth muscle of guinea-pig antrum. *J Physiol* **519**, 235–250.

He XD & Goyal RK(1993). Nitric oxide involvement in the peptide VIP-associated inhibitory junction potential in the guinea-pig ileum. *J Physiol* **461**, 485–499.

Hirst GDS, Beckett EAH, Sanders KM & Ward SM (2002*a*). Regional variation in contribution of myenteric and intramuscular interstitial cells of Cajal to generation of slow waves in mouse gastric antrum. *J Physiol* **540**, 1003–1012.

Hirst GDS, Bramich NJ, Teramoto N, Suzuki H & Edwards FR (2002*b*). Regenerative component of slow waves in the guinea-pig gastric antrum involves a delayed increase in $[Ca^{2+}]_i$ and Cl^- channels. *J Physiol* **540**, 907–919.

Hirst GDS, Dickens EJ & Edwards FR (2002*c*). Pacemaker shift in the gastric antrum of guinea-pigs produced by excitatory vagal stimulation involves intramuscular interstitial cells. *J Physiol* **541**, 917–928.

Hirst GDS & Edwards FR (2001). Generation of slow waves in the antral region of guinea-pig stomach – a stochastic process. *J Physiol* **535**, 165–180.

Itoh T, Seki N, Suzuki S, Ito S, Kajikura J & Kuriyama H (1992). Membrane hyperpolarization inhibits agonist-induced synthesis of inositol 1, 4, 5-trisphosphate in rabbit mesenteric artery. *J Physiol* **451**, 307–328.

Kito Y, Fukuta H, Yamamoto Y & Suzuki H (2002). Excitation of smooth muscles isolated from the guinea-pig gastric antrum in response to depolarization. *J Physiol* **543**, 155–167.

Lyster DJ, Bywater RAR, Taylor GS & Watson MJ (1992). Effects of a nitric oxide synthase inhibitor on non-cholinergic junction potentials in the circular muscle of the guinea pig ileum. *J Auton Nerv Sys* **41**, 187–196.

Niel JP, Bywater RAR & Taylor GS (1983). Apamin-resistant post-stimulus hyperpolarization in the circular muscle of the guinea-pig ileum. *J Auton Nerv Sys* **9**, 565–569.

Ohba M, Sakamoto Y & Tomita T (1975). The slow wave in the circular muscle of the guinea-pig stomach. *J Physiol* **253**, 505–516.

Sergeant GP, Hollywood MA, McHale NG & Thornbury KD (2001*a*). Spontaneous Ca^{2+} activated Cl^- currents in isolated urethral smooth muscle cells. *J Urol* **166**, 1161–1166.

Sergeant GP, Hollywood MA, McCloskey KD, McHale NG & Thornbury KD (2001*b*). Role of IP(3) in modulation of spontaneous activity in pacemaker cells of rabbit urethra. *Am J Physiol Cell Physiol* **280**, C1349–1356.

Suzuki H & Hirst GDS (1999). Regenerative potentials evoked in circular smooth muscle of the antral region of guinea-pig stomach. *J Physiol* **517**, 563–573.

Suzuki H, Takano H, Yamamoto Y, Komuro T, Saito M, Kato K & Mikoshiba K (2000). Properties of gastric smooth muscles obtained from mice which lack inositol trisphosphate receptor. *J Physiol* **525**, 105–111.

Suzuki H, Ward SM, Bayguinov YR, Edwards FR & Hirst GDS (2003). Involvement of intramuscular interstitial cells in nitrergic inhibition in the mouse gastric antrum. *J Physiol* **546**, 751–763.

Van Helden DF, Imtiaz MS, Nurgaliyeva K, Von Der Weid P & Dosen PJ (2000). Role of calcium stores and membrane voltage in the generation of slow wave action potentials in guinea-pig gastric pylorus. *J Physiol* **524**, 245–265.

Waniishi Y, Inoue R, Morita H, Teramoto N, Abe K & Ito Y (1998). Cyclic GMP-dependent but G-kinase-independent inhibition of Ca^{2+}-dependent Cl^- currents by NO donors in cat tracheal smooth muscle. *J Physiol* **511**, 719–731.

Ward SM, Beckett EA, Wang X, Baker F, Khoyi M & Sanders KM (2000). Interstitial cells of Cajal mediate cholinergic neurotransmission from enteric motor neurons. *J Neurosci* **20**, 1393–1403.

Ward SM, Burns AJ, Torihashi S & Sanders KM (1994). Mutation of the proto-oncogene *c-kit* blocks development of interstitial cells and electrical rhythmicity in murine intestine. *J Physiol* **480**, 91–97.

Ward SM, Dalziel HH, Bradley ME, Buxton IL, Keef K, Westfall DP & Sanders KM (1992). Involvement of cyclic GMP in non-adrenergic, non-cholinergic inhibitory neurotransmission in dog proximal colon. *Br J Pharmacol* **107**, 1075–1082.

Zhang Y & Paterson WG (2002). Role of Ca^{2+}-activated Cl^- channels and MLCK in slow IJP in opossum esophageal smooth muscle. *Am J Physiol Gastrointest Liver Physiol* **283**, G104–114.

Acknowledgements

This project was supported by a grant from the Australian NH&MRC. Dr Noriyoshi Teramoto was supported by a grant from the Ministry of Education, Science, Sports and Culture of Japan (Grant Numbers1450080 and 14-KEN-108). We are grateful to Drs N. J. Bramich and F. R. Edwards for their comments on the manuscript.